Fourier spectroscopy of a spin-orbit coupled Bose gas

Ana Valdés-Curiel, Dimitri Trypogeorgos, Erin E. Marshall, Ian B. Spielman

Joint Quantum Institute, University of Maryland and National Institute of Standards and Technology, College Park, Maryland, 20742, USA

Abstract.

We propose a time domain technique to measure the band structure of a spin-1 spin-orbit coupled Bose-Einstein condensate that relies on the Hamiltonian evolution of the system. We drive transitions at different values of detuning from Raman resonance and extract the Fourier components of the time evolution to reconstruct the spin and momentum dependent energy spectrum. We are able to map the SOC dispersion both for time independent coupling and also for a periodically driven system, which has a tunable spin-orbit coupling dispersion and a spectrum of Floquet quasi-energies, showing the robustness of our technique.

1. Introduction

Properties of materials deeply depend in their underlying band structure. Cold atoms systems offer an exciting possibility to engineer single particle dispersions that are analogues to condensed matter systems and new exotic materials, e.g. completely flat bands where interactions dominate the system, spin-orbit systems, systems with non-trivial topology [1, 2].... The ability to measure the engineered dispersions leads to a deeper understanding and paves the way to accessing new phases of matter.

The relation between the energy spectrum of a system and its dynamics is rooted in the heart of quantum mechanics. This relation has been exploited before to study spectral properties of both condensed matter [need a good cite here] and cold atoms systems [3, 4] alike. We propose a new Fourier spectroscopy technique to measure the dispersion relation of spin-orbit coupled ultra-cold atoms, which unlike previously studied techniques [5], relies only in the Hamiltonian evolution of the system and does not require any additional hardware or hyperfine states. Fourier spectroscopy relies on an atomic bare eigenstates being projected into a superposition of dressed states when a field is suddenly turned on, that evolves in time with spectral components related to the relative energies of the dressed states. Our technique can be particularly useful to study driven systems, where it is hard to predict how the different Floquet manifolds of the system couple.

We engineered a dispersion relation that has equal contributions of Rashba and Dresselhaus SOC by coupling the internal degrees of freedom of ultra-cold ^{87}Rb atoms using laser fields [6]. We study the case of time independent SOC and periodically driven SOC, which can be described by an effective time independent model with tunable SOC strength [7].

We generate the spin-orbit coupling using a pair of 'Raman' laser beams that change the spin state while imparting momentum to a spin-one atom via two photon Raman transitions [8, 9]. A uniform magnetic field $B\hat{\mathbf{e}}_z$ generates a linear Zeeman splitting of the energy levels $\hbar\omega_Z = g_F\mu_B B$, where μ_B is the Bohr magneton and g_F is the Landé g factor, and introduces a quadratic Zemen shift ϵ that shifts the energy of the $|m_F = 0\rangle$ state with respect to the $|m_F = \pm 1\rangle$ states. We couple the three states using a pair of intersecting, cross polarized Raman beams with angular frequency ω_A and $\omega_B = \omega_A + \omega_Z + \Delta_0$, where Δ_0 is an experimentally controllable detuning from four photon resonance between the $|m_F = -1\rangle$ and $|m_F = +1\rangle$ states. The Raman field couples the state $|m_F = 0,\ q_x\rangle$ to $|m_F = -1,\ q_x + 2k_L\rangle$ and to $|m_F = +1,\ q_x - 2k_L\rangle$, generating a spin change of $\delta m_F = \pm 1$ and imparting a shift in momentum of $\pm 2k_L$, where q_x denotes the quasimomentum. The geometry and wavelength of the Raman field determine the natural units of the system: the single photon recoil momentum $k_L = \frac{2\pi}{\lambda_R}\sin(\theta/2)$ and its associated recoil energy $E_L = \frac{\hbar^2 k_L^2}{2m}$.

In a frame rotating at a frequency ω_Z, and after a rotating wave approximation, the kinetic and atom-light contributions of the Hamiltonian along the recoil direction

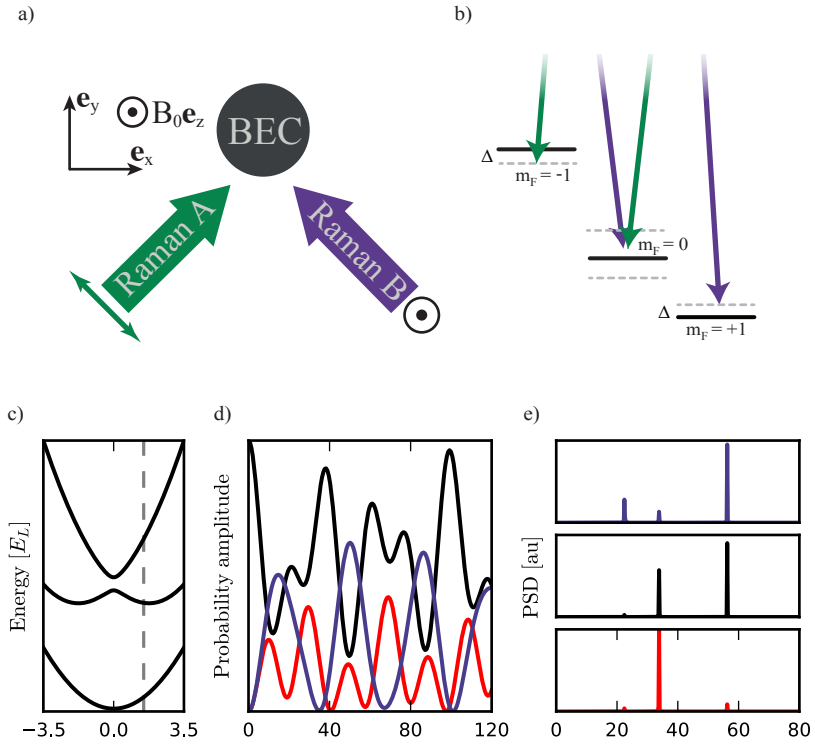

Figure 1. **c)** SOC dispersion of a spin-one system with quadratic Zeeman shift of $9E_L$ and Raman coupling $\Omega_0 = 12E_L$, initially prepared at a momentum $k_x = 2k_L$. **d)** Probability amplitude of measuring the atoms in the state $|m_F = -1,\ q_x = q_x + 2k_L\rangle$ (red), $|m_F = 0,\ q_x = q_x\rangle$ (black), and $|m_F = +1,\ q_x = q_x - 2k_L\rangle$ (blue) as a function of Raman pulsing time. **e)** Fourier transform of the probability amplitude. The three peaks in the Fourier spectra correspond to the three relative energies in the SOC dispersion for the parameters described above.

are

$$\begin{aligned}\hat{H}_x =& \frac{\hbar^2\hat{q}_x^2}{2m} + \alpha_0\hat{q}_x\hat{F}_z + 4E_L\mathbb{I} + \frac{\Omega_R}{2}\hat{F}_x] \\ &+ (-\epsilon + 4E_L)(\hat{F}_z^2 - \mathbb{I}) + \Delta_0\hat{F}_z,\end{aligned} \tag{1}$$

where $\hat{F}_{x,y,z}$ are the spin-one matrices, $\alpha_0 = \frac{\hbar^2 k_L}{m}$ is the spin-orbit coupling strength, $\Omega_R \propto E_A^\star E_B$ and the Raman coupling strength which is proportional to the field intensity.

Figure 1c shows the typical band structure as a function of quasimomentum that results of diagonalizing the Hamiltonian $\hat{H}_x$ for a negative quadratic Zeeman shift $|\epsilon| > 4E_L$. The ground state band is pushed down with respect to the higher excited bands, and it can be well described by a harmonic potential as there are no crossings with the higher bands.

1.1. Fourier spectroscopy of spin-orbit coupled atoms

We can directly measure the dispersion relation of a system of spin-one, spin-orbit coupled atoms by studying the Hamiltonian evolution of the system.

We start with bare atoms in the $|m_F = 0,\ k_x\rangle$ state. When a Raman field is suddenly turned on, the initial state is projected into the Raman dressed state basis, and continues to evolve $|m_F = 0, q_x\rangle \rightarrow \sum_{i=1}^{3} c_i e^{i\omega_i t}|\psi_i\rangle$, where $\omega_i = E_i/\hbar$ are the angular frequencies associated to the dressed state energies and $|\psi_i\rangle$, the dressed eigenstates, are linear combinations of $|m_F = 0,\ q_x = k_x\rangle$ and $|m_F = \pm 1,\ q_x = k_x \mp 2k_L\rangle$. We then turn off the Raman field and image the atoms, which projects the system back into the bare basis $|m_F = 0,\ q_x = k_x\rangle$, $|m_F = \pm 1,\ q_x = k_x \mp 2k_L\rangle$. The probability amplitude of measuring atoms in an m_F state after evolving for a time t oscillates at frequencies given by the difference in the dressed state energies $P_{m_F}(t) = \sum_{i \neq j} 2c_{ij} \cos((\omega_i - \omega_j)t)$.

The Fourier spectroscopy technique relies in directly measuring the probability amplitude as a function of evolution time and extracting the relative energies of the system using a Fourier transform, as shown in figure 2d,e.

The method described above so far only allows us to measure relative energies and we must add a known energy reference if we want to recover the dispersion relation. We can do so by measuring the effective mass $m^\star = \hbar^2[\frac{d^2E(k_x)}{dk_x}]^{-1}$ of the nearly quadratic lowest branch of the dispersion, and then shifting the measured frequencies accordingly.

We can map the full spin and momentum dependent band structure of the spin-orbit coupled system by repeating this procedure for different initial momentum states, however, it may not be as straightforward to reliably prepare an arbitrary momentum state in the lab. The measurement however can be simplified by noticing that a non-moving atom cloud in the laboratory reference frame dressed by a laser field with non-zero detuning is equivalent to a moving cloud with a resonant field the cloud reference frame. This can be explicitly seen in the Hamiltonian 1 by looking at the detuning term $\Delta_0 \hat{F}_z$ and the momentum term $\alpha_0 \hat{q}_x \hat{F}_z$, which have the same effect in the relative energies. There is an additional Doppler shift associated with the transformation between reference frames, which gets canceled when we look at the energy differences. Therefore, for the purpose of our experiments, momentum and detuning are equivalent up to a numerical factor: $\Delta_0/E_R = 4q_x/k_R$, and we can measure by preparing a zero momentum state and measuring the probability amplitude for different values of Raman detuning Δ_0.

1.2. Spectroscopy of a time dependent system

A time evolution based spectroscopy is ideal to study the energy spectrum of more complex time dependent systems. A particularly interesting case is that of periodically driven systems [7, 10, 11], which can be described by effective coupling terms in the Hamiltonian that arise from averaging the fast dynamics of the system.

We will focus on the case of a spin-1 spin-orbit coupled system that is coupled by

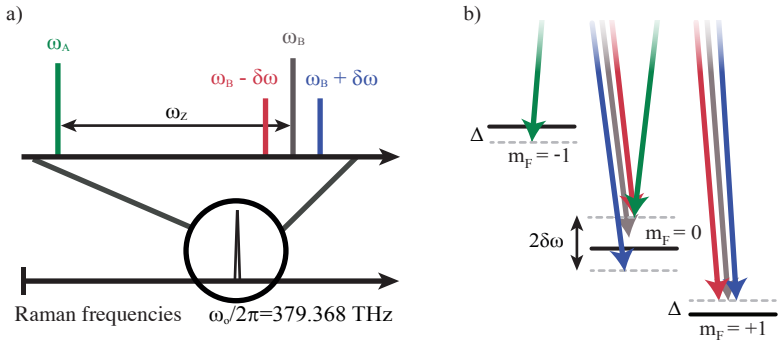

Figure 2. We use a multiple frequency Raman beam with up to 3 frequencies that gives rise to a system with tunable spin-orbit coupling. **(a)** Frequency components in each Raman beam **(b)** The combination of a blue and red sideband are at four photon resonance between the $|m_F = +1\rangle$ and $|m_F = -1\rangle$ state and there are two possible paths to couple these states.

a multiple frequency Raman field, as shown in Fig 2. The interference of the multiple frequencies leads to a periodic amplitude modulation in the field and an effective Floquet Hamiltonian that has tunable spin-orbit coupling [7].

We add two sidebands to one Raman beam at angular frequencies $\omega = \omega_L + \omega_Z + \Delta_0 \pm \delta\omega$. The Hamiltonian in Eq.1 remains unchanged, except for the coupling strength that takes the form $\Omega_R(t) = \Omega_0 + \Omega\cos(\delta\omega t)$. Our periodically driven system is well described by Floquet theory: the eigenstates are of the form $|\Psi_\epsilon(t)\rangle = e^{-i\epsilon t}\sum_{l=-\infty}^{+\infty} e^{i\epsilon t}|\psi_{\epsilon,l}(t)\rangle$ where $|\psi_{\epsilon,l}(t)\rangle$ are time-periodic states, whose energies differ by integer multiples of the driving frequency.

The time evolution of the system after one driving cycle can also be described in terms of an effective time-independent Hamiltonian $e^{iT\hat{H}_{eff}}$. If $\delta\omega \gg 4E_L$, this effective Floquet Hamiltonian retains the form of 1 with renormalized coefficients, and an additional term that couples the $m_f = -1$ and $m_f = +1$ states:

$$\begin{aligned}\hat{H} =& \frac{\hbar^2\hat{k}^2}{2m} + \alpha\hat{k}\hat{F}_z + 4E_L\mathbb{I} + \frac{\Omega_0}{2}\hat{F}_x \\ &+ \frac{\tilde{\Omega}}{2}\hat{F}_{xz} + (\tilde{\epsilon} + 4E_L)(\hat{F}_z^2 - \mathbb{I}) + \tilde{\Delta}\hat{F}_z,\end{aligned} \tag{2}$$

with $\alpha = J_0(\Omega/2\delta\omega)\alpha_0$, $\tilde{\Omega} = \frac{1}{4}(\epsilon + 4E_L)(J_0(\Omega/\delta\omega) - 1)$, $\Delta = J_0(\Omega/2\delta\omega)\Delta_0$, and $\tilde{\epsilon} = \frac{1}{4}(4E_L - \epsilon) - \frac{1}{4}(4E_L + 3\epsilon)J_0(\Omega/\delta\omega)$, and J_0 the zeroth order Bessel function of the first kind.

If the quadratic Zeeman shift and the driving frequency are large compared to the recoil energy $|\epsilon|, \delta\omega > 4E_L$, the Hamiltonian described above can be approximated by an effective spin 1/2, spin-orbit coupled system,with tunable spin-orbit coupling:

the state $|m_F = +1,\ q_x = k_x - 2J_0(\Omega/2\delta\omega)k_R\rangle$ is coupled to the $|m_F = -1,\ q_x = k_x + 2J_0(\Omega/2\delta\omega)k_R\rangle$ with coupling strength $\Omega' = \tilde{\Omega} + \hbar\Omega_0^2/2\tilde{\epsilon}$[12].

This model is good to describe the energies within one Floquet manifold, however, if the coupling strength becomes comparable to the driving frequency Ω_0, $\Omega \geq \delta\omega$, rotating wave type approximations (neglecting fast terms) break down, and the time evolution of the system becomes more complex. A signature of this is the appearance of higher frequency Fourier components in the probability amplitude, spaced by $\delta\omega$ from the lowest 3 energy levels. We expect the band structure from this type of system to be more complex, but easily interpreted by understanding the periodically repeating structure of the Floquet quasi-energies.

2. Experiment

We are interested in measuring the SOC dispersion for three different types of coupling schemes: (i) A time independent spin-orbit coupled system, $\Omega_0 \neq 0$ and $\Omega = 0$, (ii) for a periodically driven spin-orbit coupled system with no DC offset $\Omega \neq 0$ and $\Omega_0 = 0$, and (iii) A time periodically driven spin-orbit coupled system with a DC offset $\Omega \neq 0$ and $\Omega_0 \neq 0$.

2.1. Spectroscopy experimental sequence

We start our experiments with a Rb^{87} Bose-Einstein condensate [13] (BEC) with $N \approx 4\times10^4$ (measure) atoms in the $|F = 1, m_F = 0\rangle$ state, confined in a 1064 nm crossed optical dipole trap, with trapping frequencies $(\omega_x, \omega_y, \omega_z) = 2\pi(42(3), 34(2), 133(3))$ Hz. We break the degeneracy between the m_F magnetic sub-levels by applying a 17.0556 G bias field along the z axis, which produces a Zeeman splitting of 12 MHz and a quadratic Zeeman shift that lowers the energy of the $|F = 1, m_F = 0\rangle$ state by 20.9851 kHz. We adiabatically prepare our BEC in the $|m_F = 0\rangle$ by slowly ramping the bias field while applying a 12 MHz radio-frequency field. We then apply a pair of microwave pulses that serve to monitor and stabilize the bias field and. We generate spin-orbit coupling between the magnetic sub levels with a pair of intersecting, cross-polarized Raman beams, with wavelength $\lambda = 790.024nm$ propagating along $\mathbf{e}_x + \mathbf{y}$ and $\mathbf{e}_x - \mathbf{e}_y$ as shown in Fig 1a. We offset the frequency of the beams using two acusto optic modulators (AOMs), one of them driven by a superposition of up to three different frequencies. On resonance, the laser frequencies satisfy the condition $\omega_A - \omega_B = \omega_A - \frac{\omega_{B+}+\omega_{B-}}{2} = \omega_Z$, and we change the Raman detuning Δ_0 by keeping the magnetic field constant and changing the value of the frequency ω_A.

To get our probability amplitude measurements, we keep the detuning value Δ_0 fixed and pulse the Raman beams on for time intervals between 5 μs and up to 900 μs. For the time independent SOC measurements (case (i)) we take a total of 120 different pulses, for the periodically driven SOC measurements (cases (ii) and (iii)) which require better resolution and bandwidth, we take a total of 180 pulses. After pulsing the Raman

we release our atoms from the optical dipole trap and let them fall for a 21 ms time of flight (TOF) time before and apply a spin-dependent force using magnetic field gradient. Our absorption images reveal the atoms spin and momentum distribution, from which we can extract the probability amplitudes by counting the fractional number of atoms in each spin and quasimomentum state. We repeat this procedure for values of Raman detuning within the interval $\pm 12 E_L$ which corresponds to quasimomentum values within $\pm 3 k_L$.

The time dependent SOC measurements additionally required phase stability between the 3 frequency components in the Raman B field. We set all the relative phases to zero at the beginning of each pulse and kept it constant throughout our experiments. We made the choice of zero relative phase as it maximizes the effective couplings Ω and Ω_0 for a given field intensity. For a more detailed discussion of the effect of the relative phases see the Appendix section (?).

2.2. Effective mass measurement

We measure the atom's ground state effective mass by adiabatically preparing our BECs in the lowest eigenstate and inducing dipole oscillations.The effective mass $m^\star$ of the dressed atoms is related to the bare mass m and the bare and dressed trapping frequencies ω and $\omega^\star$ by the ratio $m^\star/m = \sqrt{\omega^\star/\omega}$. We prepare our system in the $|m_F = 0,\ k_x = 0\rangle$ and adiabatically turn on the Raman in ≈ 10 ms while also ramping the detuning to a non-zero value, around $0.5 E_R$. Our system does not have the capability to dynamically change the laser frequency while maintaining phase stability, so unlike the pulsing experiments, we ramped the magnetic field to change the resonance conditions. This detuning shifts the minima in the ground state energy away from zero quasi-momentum. We then suddenly snap the field back to resonance which changes the equilibrium conditions of the system and excites the dipole mode of our optical dipole trap. To measure the bare state frequency, we use the Raman beams to initially excite the dipole mode of the trap but we quickly turn off the field (~ 1 ms) and let the BEC continue to oscillate in the unmodified dipole potential.

For this set of measurements we modified our trapping frequencies to $(\omega_x, \omega_y, \omega_z) = 2\pi(35.9, 32.5, xx)$ Hz so that they were nominally symmetric along the $x - y$ plane.

2.3. Magnetic field stabilization

We stabilized the magnetic field and measured fluctuations about the desired set point by applying a pair of microwave pulses with frequencies close to resonance from the $5^2\mathrm{S}_{1/2}$ $F = 2$ state, and imaging the in-situ the population transfered by each pulse.

We first prepare our BEC in the $|F = 1, m_f = 0\rangle$ state and apply a 17.0556 G bias filed along the z axis. We then apply a pair of $250\mu s$ microwave pulses close to $6.83 GHz$ that transfers about 10% of the atoms into the $F = 2$ manifold. The pulses were detuned by ± 2 kHz from the $|F = 1, m_F = 0\rangle \leftrightarrow |F = 2, m_F = 1\rangle$ transition and were spaced in time by 2 periods of 60 Hz. We image the atoms transfered into $F = 2$

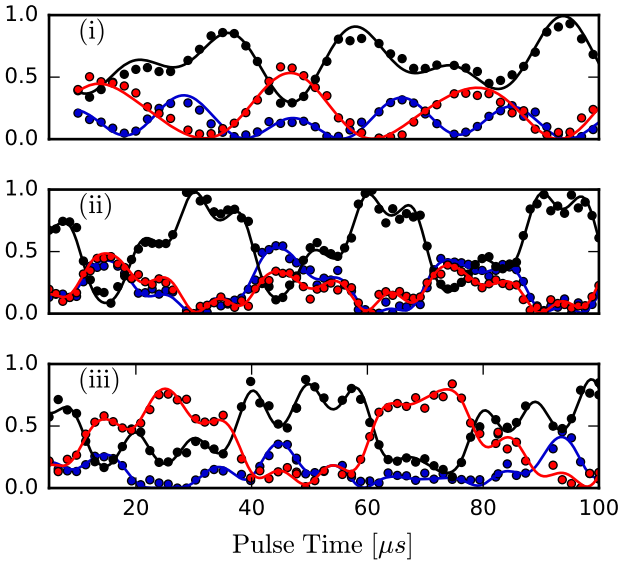

Figure 3. Time evolution of the BEC for Raman pulsing times between 5 and 10 μs, for different spin orbit coupling regimes: **(i)** $\Omega_0 = 9.9E_L$, $\Omega = 04$, $\Delta = 5.8E_L$, **(ii)** $\Omega_0 = 0$, $\Omega = 8.6E_L$, $\Delta = -0.7E_L$, and **(iii)** $\Omega_0 = 1.5E_L$, $\Omega = 8.4E_L$, $\Delta = -4.7E_L$

non-destructively using absorption imaging without repumping light. The imbalance in the number of atoms transferred by each pulse gives us a 4 kHz wide error signal that we use both to feed forward our bias coils for active field stabilization, and also to keep track of the magnetic fields at each shot. We trigger our sequence to the line and both the microwave and Raman pulses are timed at integer periods of 60 Hz and performed at the zero-derivative point of the 60 Hz curve in order to minimize additional magnetic field fluctuations

3. Results

We mapped the band structure of our spin-orbit coupled atoms for three different types of coupling. A fit our experimentally calculated probability amplitudes to the Hamiltonian evolution shows that our system is well described by the Hamiltonian 1 with either Ω time dependent or independent. The fit can also be used as an additional calibration method to extract the Raman coupling terms Ω and Ω_0 and the detuning from Raman resonance Δ. Figure 3 shows representative traces for the time evolution of our system for the three cases outlined above. These calibrations along with the information gained from the images of atoms out-coupled with microwaves guaranteed that we were indeed at the correct detuning from Raman resonance and that the Raman coupling strength remained nominally constant throughout our measurements.

The time evolution shows higher frequency components for cases (ii) and (iii), as expected from the Floquet quasi-energy spectrum, since the Raman coupling strength

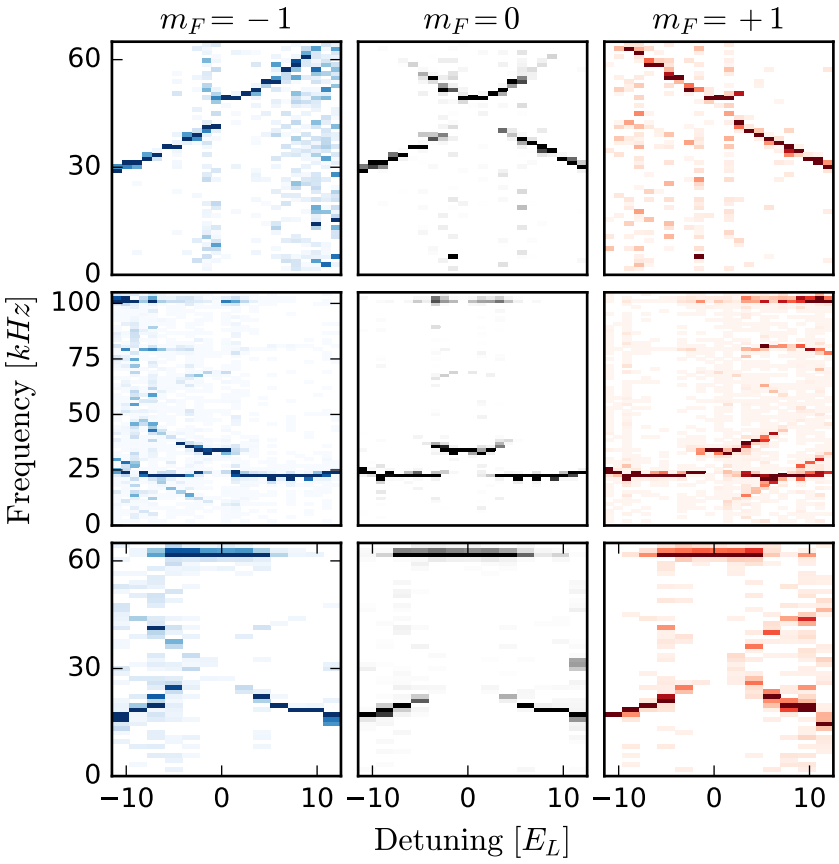

Figure 4. Power spectral density of the experimentally measured probability amplitudes for for different spin orbit coupling regimes: **(i)** $\Omega_0 = 9.9E_L$, $\Omega = 04$, $\Delta = 5.8E_L$, **(ii)** $\Omega_0 = 0$, $\Omega = 8.6E_L$, $\Delta = -0.7E_L$, and **(iii)** $\Omega_0 = 1.5E_L$, $\Omega = 8.4E_L$, $\Delta = -4.7E_L$

Ω, Ω_R is comparable to the separation between the Floquet manifolds $\delta\omega$.

We use a not-uniform fast Fourier transform algorithm (NUFFT) which allows us to get the power spectral density for data points that are not necessarily evenly spaced in time, as required by regular FFT algorithms. Our experimental sequences have in principle evenly spaced pulsing times, but in practice we need to take into account data points that are sometimes missing for reasons beyond our control. Figure 4 shows the power spectral density (PSD) of the time evolution of each m_F state. Each vertical cut is normalized to the highest peak of the three spin states.

For cases (ii) and (iii) we notice peaks at constant frequencies of $\delta\omega$ and $2\delta\omega$, independently of the Raman detuning, and a structure that is symmetric about the frequencies $2\pi f = \delta\omega/2$ and $2\pi f = \delta\omega$ which can be interpreted as the atoms coupling to the neighboring Floquet manifolds.

Our system also has dark states at $\Delta_0 = 0$ which can be noted by the missing peaks in the PSD. Since there are eigenstates of the Raman dressed Hamiltonian that never get populated, the time evolution of the system does not have the frequency components

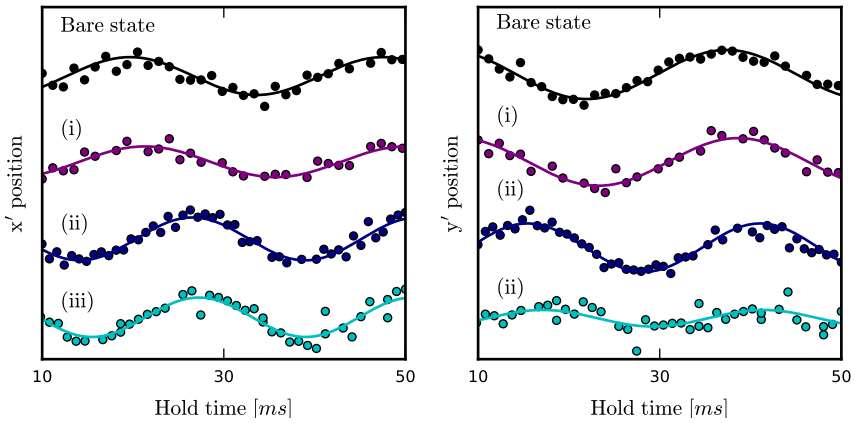

Figure 5. Oscillation of the BEC in the dipole trap along the directions $\mathbf{e}_{x'}$ and $\mathbf{e}_{y'}$ defiend by the propagation of the dipole tap beams. The traces have been shifted so that it is easier to appreciate the change in the motion for each coupling regime.

related to the missing eigenstates. The presence of the dark states in the system is in good agreement with theory.

To calculate the effective mass we fitted sinusoids to the sloshing motion of our atoms in the dipole trap and extracted the frequency of oscillation. Our Raman beams are co-propagating with the optical dipole trap beams, therefore the direction of the measured dipole trap frequencies is at a 45° angle with respect to the direction of k_L. The kinetic and harmonic terms in the Hamiltonian are

$$\hat{H}_\perp = \frac{1}{2m^\star}k_x^2 + \frac{1}{2m}k_y^2 + \frac{m}{2}[\omega_{x'}^2 x'^2 m + \omega_y'^2 y'^2] \tag{3}$$

with $\mathbf{e}_{x'} = \frac{\mathbf{e}_x+\mathbf{e}_y}{\sqrt{2}}$ and $\mathbf{e}_{y'} = \frac{\mathbf{e}_x-\mathbf{e}_y}{\sqrt{2}}$. For $\omega_{x'} = \omega_{y'}$ a simple rotation yields a trapping frequency along the Raman direction $\omega_x = \sqrt{\omega_x^2 + \omega_y^2}$. Figure 6 shows the dipole oscillations of our BECs along the $\mathbf{e}_{x'}$ and $\mathbf{e}_{x'}$ directions for the three different coupling regimes we are studying, as well as the bare state motion.

After rescaling the horizontal axis from recoil energy to recoil momentum and subtracting the effective mass, we can finally obtain the characteristic dispersion of a spin orbit coupled system as seen in Figure 6. We have additionally overlapped the eigen energies, which are in good agreement with our spectroscopy measurements.

4. Discussion

Heating due to scattering of spontaneously emitted photons is always present in our system. It is also well known that heating is present in periodically driven systems, and while it can be minimized by increasing the driving frequency, it in exchange requires more Raman power to tune the spin-orbit coupling strength. The time scales of our pulsing experiments never exceeded 900 μs which is small compared to the lifetime of our system.

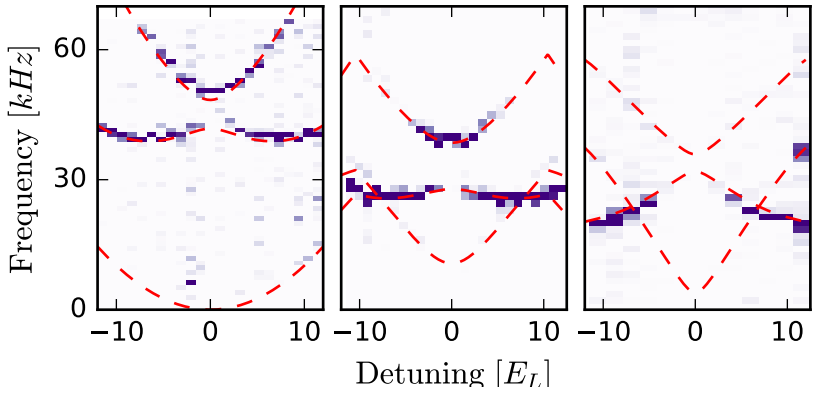

Figure 6. This figure needs some love but this is more or less the idea. Only the first panel has the effective mass substracted, other 2 are energy differences. I was thinking of maybe making the theory lines thicker to include uncertainties.

In conclusion, we can measure the spin and momentum dependent dispersion relation for a spin-1 spin-orbit coupled BEC using our Fourier spectroscopy technique. When used to study periodically driven systems, we are able tp see a rich spectrum that arises from the Floquet quasi-energies. This method allows one to measure the spectrum of a system just by looking at the time evolution without the need of fitting to a complicated model and is good for any effective three level system with a quadratic branch in the spectrum. This technique might prove particularly useful to probe the spin-resolved energy dispersion of atoms in the presence of Rashba spin-orbit coupling using newly proposed schemes to generate this type of coupling without the use of excited states [**?**] and could lead to a better understanding of new topological materials.

[1] Lindner N H, Refael G and Galitski V 2011 *Nature Physics* **7** 490–495 ISSN 1745-2473 URL `http://www.nature.com.proxy-um.researchport.umd.edu/nphys/journal/v7/n6/full/nphys1926.html`

[2] Radić J, Natu S S and Galitski V 2015 *Physical Review A* **91** 063634 URL `http://link.aps.org/doi/10.1103/PhysRevA.91.063634`

[3] Yoshimura B, Campbell W C and Freericks J K 2014 *Physical Review A* **90** 062334 URL `http://link.aps.org/doi/10.1103/PhysRevA.90.062334`

[4] Wang L, Zhang H, Zhang L, Raithel G, Zhao J and Jia S 2015 *Physical Review A* **92** 033619 URL `http://link.aps.org/doi/10.1103/PhysRevA.92.033619`

[5] Cheuk L W, Sommer A T, Hadzibabic Z, Yefsah T, Bakr W S and Zwierlein M W 2012 *Physical Review Letters* **109** 095302 URL `http://link.aps.org/doi/10.1103/PhysRevLett.109.095302`

[6] Dalibard J, Gerbier F, Juzeliūnas G and Öhberg P 2011 *Reviews of Modern Physics* **83** 1523–1543 URL `http://link.aps.org/doi/10.1103/RevModPhys.83.1523`

[7] Jiménez-García K, LeBlanc L, Williams R, Beeler M, Qu C, Gong M, Zhang C and Spielman I 2015 *Physical Review Letters* **114** 125301 URL `http://link.aps.org/doi/10.1103/PhysRevLett.114.125301`

[8] Lan Z and Öhberg P 2014 *Physical Review A* **89** 023630 URL `http://link.aps.org/doi/10.1103/PhysRevA.89.023630`

[9] Campbell D L, Price R M, Putra A, Valdés-Curiel A, Trypogeorgos D and Spielman I B 2015 *arXiv:1501.05984 [cond-mat, physics:physics]* ArXiv: 1501.05984 URL `http://arxiv.org/abs/1501.05984`

[10] Eckardt A, Weiss C and Holthaus M 2005 *Physical Review Letters* **95** 260404 URL `http://link.aps.org/doi/10.1103/PhysRevLett.95.260404`

[11] Goldman N and Dalibard J 2014 *Physical Review X* **4** 031027 URL http://link.aps.org/doi/10.1103/PhysRevX.4.031027
[12] L J LeBlanc M C B 2013 *New Journal of Physics* **15** ISSN 1367-2630
[13] Lin Y J, Perry A R, Compton R L, Spielman I B and Porto J V 2009 *Physical Review A* **79** 063631 URL http://link.aps.org/doi/10.1103/PhysRevA.79.063631

5. Appendix A

5.1. Effective SOC Hamiltonian

Maybe I will put a more detailed derivation of the theory here, not sure.